



Heterogeneous & Homogeneous & Bio- & Nano-

CHEM **CAT** CHEM

CATALYSIS

Accepted Article

Title: Pt Nanoparticles Supported over Porous Porphyrin Nanospheres for Chemoselective Hydrogenation Reactions

Authors: Arindam Modak, Piyali Bhanja, and Asim Bhaumik

This manuscript has been accepted after peer review and appears as an Accepted Article online prior to editing, proofing, and formal publication of the final Version of Record (VoR). This work is currently citable by using the Digital Object Identifier (DOI) given below. The VoR will be published online in Early View as soon as possible and may be different to this Accepted Article as a result of editing. Readers should obtain the VoR from the journal website shown below when it is published to ensure accuracy of information. The authors are responsible for the content of this Accepted Article.

To be cited as: *ChemCatChem* 10.1002/cctc.201802108

Link to VoR: <http://dx.doi.org/10.1002/cctc.201802108>

WILEY-VCH

www.chemcatchem.org



DOI: 10.1002/cctc.200((will be filled in by the editorial staff))

Pt Nanoparticles Supported over Porous Porphyrin Nanospheres for Chemoselective Hydrogenation Reactions

Arindam Modak,^{*[a,b]} Piyali Bhanja^[a] and Asim Bhaumik^{*[a]}

Optimizing the chemoselectivity in a chemical reaction catalyzed by metallic nanoparticles (NPs) hosted over a solid support is a big challenge, especially in the context of the sustainability of the process. Here we showed that chemoselectivity in the hydrogenation of 4-nitrostyrene can be tailored on Pt-loaded porphyrin nanospheres through the functionalization with sulfonic acid groups at the catalyst surface. 4-Nitrostyrene is transformed to 4-aminostyrene over sulfonated Pt-POP-SO₃H, with ~77.8% selectivity at conversion of

~90%, whereas the pristine catalyst selectively produced ~80% 4-ethylnitrobenzene at almost complete conversion level. The reversal of the selectivity could be attributed to the effect of the introduction of sulfonic acid group over the supported Pt NPs. Presence of sulfonic acid groups in the functionalized Pt-porphyrin material has been confirmed from XPS, FT-IR and elemental analysis data. Moreover, these catalysts are recyclable, suggesting their durability and chemical-stability for long-term sustainable operations.

Introduction

Supported metallic NPs are promising catalysts for a wide variety of chemical and electrochemical reactions.^[1] Therefore, development of highly active and selective heterogeneous metal catalysts have attracted a huge interest over the years. Generally, selectivity for a desired product in a chemical reaction can be optimized by modulating the size, shape, dispersibility, poisoning or alloying with other metals to promote metal-support interaction.^[2] It has been reported that organic ligands grafted on inorganic supports (silica, alumina) are very useful for tuning the catalytic activity and selectivity of supported noble metals.^[3] But ligands can often break from the support and/or consumed during the catalyst recovery in the recycling process, which suggested continuous monitoring of the catalyst surface. Further, pore blocking by the organic ligands prevents the smooth progress of reaction by hindering the diffusion of reactants and products through pore channels of the catalyst. Therefore heterogeneous catalyst comprising organic porous polymer as a single support could be advantageous over organic-inorganic hybrid supports.^[4]

As a host matrix, metal-organic-frameworks (MOFs) can act as a good support for metallic NPs, which could take part in the catalytic reactions with high activity and selectivity for the desired products.^[5] But, these coordination polymers often become unstable under the liquid phase reaction conditions, which are carried out in the presence of water. As supplement to MOFs, porous organic polymers (POPs)^[6] are well recognized as solid catalyst because of their robust framework, high surface area and tenability of reactive functional groups at its surface. The stability of POPs during liquid phase catalysis have made them as an emerging class of solid-support.^[6] Although N-containing POPs enhances interaction with noble metals and prevents aggregation and improves durability, but agglomeration of NPs after several cycles cannot be ruled out.^[7] Few years ago we developed porphyrin-based porous organic polymer (Fe-POPs) support having high activity and robustness in stabilizing Pd NPs for carrying out a series of C-C cross-coupling reactions.^[8] Fe-POPs thus produced in one-pot bottom-up approach, showed high yield, good Brunauer-Emmett-Teller (BET) surface area along with large number of nitrogen sites for anchoring and stabilizing metal nanoparticles. High yield synthesis of Fe-POPs could be promising for useful applications of this material as support for heterogeneous catalyst. With this advantage in mind, we have employed Fe-POP-1 as support for loading of ca. 2-3 nm size Pt nanoparticles at its surface and the catalyst thus produced, named as Pt-POP. Pt-POP has been employed for the catalytic hydrogenation of 4-nitrostyrene and acetophenone. Under this circumstances, Pt-POP showed excellent catalytic activity (~100% conversion), together with ~80% selectivity for the synthesis of 4-ethylnitrobenzene from 4-nitrostyrene, without showing any reduction to 4-aminostyrene. It is worthy to mention that nitrostyrene hydrogenation is a surface sensitive reaction, which can be controlled by proper modification of the catalyst surface with thiol, Zn and Au nanoclusters.^[9] Thus, we have attempted to explore the

[a] Dr. A. Modak, Dr. P. Bhanja, Prof. A. Bhaumik
School of Materials Science
Indian Association for the Cultivation of Science
2A & B, Raja S.C. Mullick Road, Jadavpur, Kolkata- 700032, India
Fax: (+91) 33-2473-2805
E-mail: msab@iacs.res.in

[b] Dr. A. Modak
Technical Research Centre
S. N. Bose National Centre for Basic Sciences,
Block - JD, Sector-III, Salt Lake, Kolkata -700106,
India
E-mail: arindam_modak_2006@yahoo.co.in

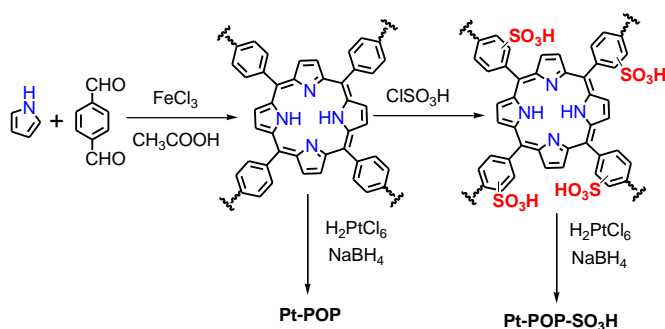
Supporting information for this article is available on the WWW under <http://dx.doi.org/10.1002/cctc.200xxxxx>

possibility of other hydrogenation products from 4-nitrostyrene by modifying the surface of the parent porous polymer through post-synthetic chemical modification. Thus, we have incorporated sulfonic acid groups at the POP surface through one-step treatment with chlorosulfonic acid as introduction of sulfur-sites often influence the catalytic activity and selectivity of metallic NPs by either electronically or geometrically.^[10]

It is noteworthy to mention that covalent grafting of sulfonic acid groups at the porous polymer surface is often quite advantageous over the non-covalent impregnation,^[9] which resulted leaching of the active metal sites from the material surface during prolonged catalytic operations. Therefore, we foresee the advantages of sulfonic acid embedded Pt-POP as stable and durable nanocatalyst. Again, the surface modification in controlling the selectivity for the catalytic processes are mostly accomplished over inorganic supports like zeolites, AlPOs, metal oxides, mesoporous materials, ZnAl-hydrotalcite, etc. Porous organic polymers can offer huge scope as support in selective hydrogenation reactions due to the change in metal-support interactions after surface modification. Here, we first showed the utility of porous organic polymer as support in heterogeneous catalysis after covalent modification with $-\text{SO}_3\text{H}$ group in selective hydrogenation reactions. Our results could open new avenue for the functionalized porous polymers as catalyst for the fine chemicals synthesis without the involvement of protection and de-protection steps in designing target organic molecules.

Results and Discussion

1. Synthesis and Characterization



Scheme 1. Schematic representation for the formation of Pt-POP and Pt-POP- SO_3H .

Porphyrin functionalized POP was prepared from one-step bottom up approach using the condensation reaction between pyrrole and terephthalaldehyde following our previous report.^[8a] Pt NPs were loaded on POP through impregnation-reduction method using H_2PtCl_6 as Pt source as shown in Scheme 1. Initially Pt-POP was characterized from powder X-ray diffraction (PXRD, Figure 1a), which showed the presence of several small intensity peaks at $2\theta = 33^\circ, 35.3^\circ, 54^\circ$ corresponding to the formation of Pt NPs at POP surface. Additionally, a broad peak at $2\theta = 25^\circ$ is seen, suggesting the amorphous nature of the POP support.^[11] The Pt NPs are quite uniformly distributed at the surface of the sulfonic acid

functionalized POP, suggesting that acid sites could act in a synergistic manner along with Pt NPs bound at the polymer matrix.

Thermogravimetric analysis has been performed to understand the thermal stability of Pt-POP and Pt-POP- SO_3H materials. As shown in Figure 1b, Pt-POP is stable upto 250°C with weight loss of $\sim 10\%$, while the sulfonic acid functionalized POP showed little decrease in thermal stability. Pt-POP- SO_3H exhibited $\sim 10\%$ weight loss at 230°C . The lower stability of Pt-POP- SO_3H than Pt-POP might be due to the presence of labile $-\text{SO}_3\text{H}$ groups bound at the polymer matrix. Surface area and porous characteristics of Pt-POP catalyst has been measured from N_2 adsorption-desorption analysis (Figure 1c). The adsorption/desorption isotherms of Pt-POP and Pt-POP- SO_3H clearly suggested the predominant microporosity owing to the steep rise of N_2 uptake at low P/P_0 (0-0.2). BET surface area for Pt-POP and Pt-POP- SO_3H were 680 and $620\text{ m}^2\text{ g}^{-1}$, respectively, which is considerably lower than the host Fe-POP-1 polymer ($875\text{ m}^2\text{ g}^{-1}$).^[8a] This could be attributed to the loading of Pt of higher atomic mass in these samples followed by $-\text{SO}_3\text{H}$ groups. Pore size distribution plots of these materials suggested the existence of mainly small micropores at $\sim 0.5\text{ nm}$ as well as inter-particle pores at $1-1.5\text{ nm}$ dimension (Figure 1d). With respect to total pore volume ($0.4\text{ cm}^3\text{ g}^{-1}$), micropore volume was $0.2\text{ cm}^3\text{ g}^{-1}$, suggesting that $\sim 50\%$ of total pores are inter-particle pores. From TEM images (Figure 2), we can easily estimate the size of Pt is about $\sim 2-3\text{ nm}$, which are evenly distributed at POP surface. The growth of small Pt NPs at POP surface could be attributed due to their stabilization by porphyrin ring and only the external porphyrin surfaces might be available for binding with Pt. In this context, it is pertinent to mention that the functional polymers containing nitrogen sites are useful scaffold for stabilizing well-dispersed metal NPs at the surface.^[12] TEM images of Pt NPs of the modified Pt-POP- SO_3H are also shown in Figure 3, which demonstrated the presence of slightly entangled Pt-sites that is in accordance with Pt in contact with organic thiols.^[9] Furthermore, the crystal fringes and the SAED images are also seen from Figure 3, indicating that the crystalline Pt NPs exists simultaneously with the acidic $-\text{SO}_3\text{H}$ groups.

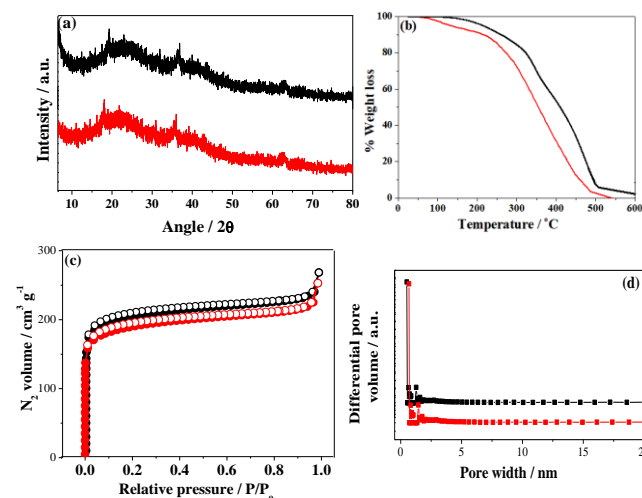


Figure 1. Powder X-ray diffraction pattern (a); TGA plots (b); N_2 adsorption (solid) desorption (hollow) isotherms (c) and NLDFT pore size distribution (d) of Pt-POP (black) and Pt-POP- SO_3H (red)

Quantitative analysis using acid-base titration suggested the presence of ~3.4 wt% $-\text{SO}_3\text{H}$ groups in Pt-POP- SO_3H . Further, the presence of sulfonic acids in Pt-POP- SO_3H has also been confirmed from the S (2p) XPS spectrum (Figure 4a), where the doublet S (2p) peaks appears at 167.4-168 eV. Deconvoluted XPS of S (2p) is shown in Figure 4b, which splits into several sites as, sulphinate ($-\text{SO}_3\text{H}$, 168.1 eV) and

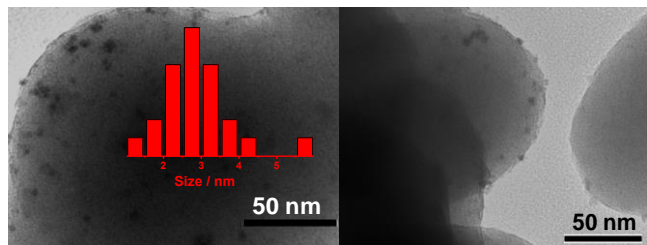


Figure 2. (a) TEM images of Pt in Pt-POP (size distribution of Pt is shown in the inset)

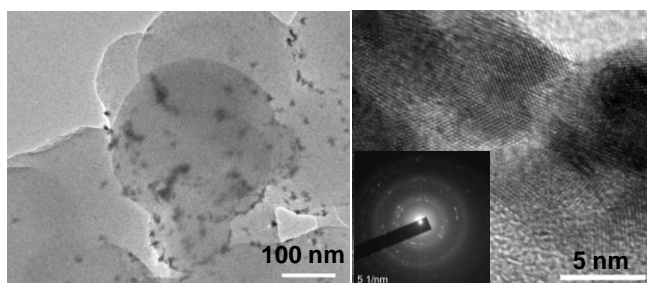


Figure 3. HR TEM images of Pt-POP- SO_3H . SAED pattern is shown in the inset.

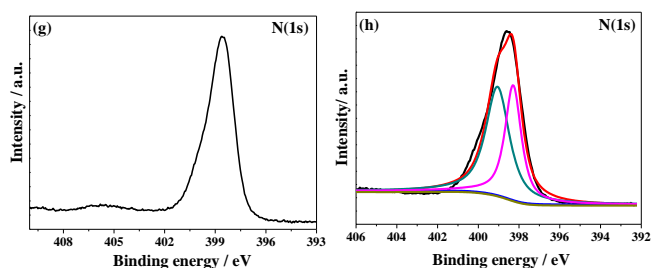
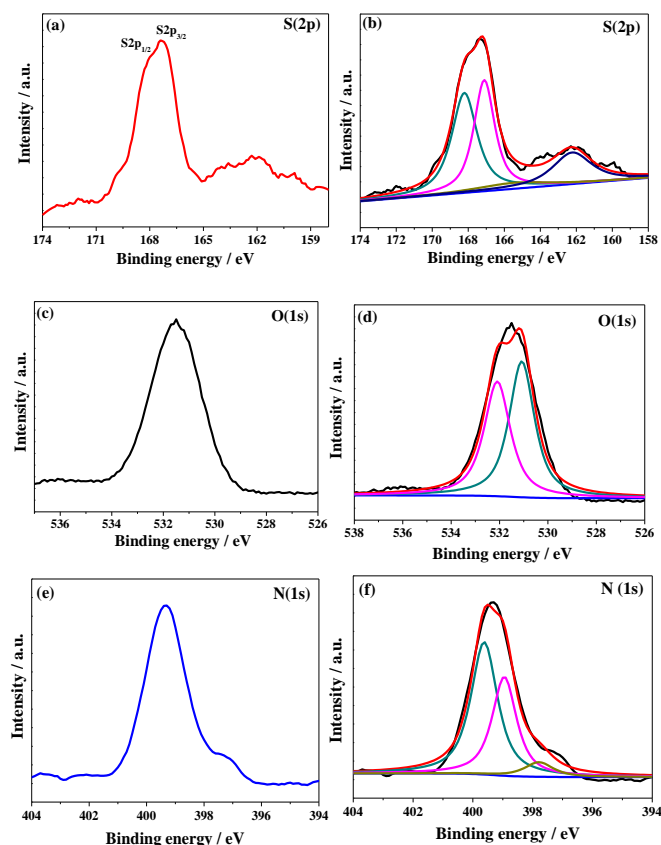


Figure 4. XPS spectra of Pt-POP- SO_3H (a-f); Pt-POP (g-h)

sulphide ($-\text{SO}_2-$, 167.3 eV).^[13] Additionally, a broad shoulder at 164-160 eV is also seen, which can be assigned due to the presence of small amount of organic sulphide (R-S-R). This XPS investigation clearly signifies the successful grafting of organic sulfonic acid. Again, the O (1s) spectrum of Pt-POP- SO_3H is given in Figure 4c, which is centered at 531.5 eV. However, this peak can be deconvoluted into two peaks at 531.2 eV for S=O and at 532 eV, corresponding to S-OH species (Figure 4d).^[14] Therefore, O (1s) XPS result confirmed the grafting of sulfonic acid groups. On the other hand, N (1s) XPS spectra of Pt-POP- SO_3H has been shown in Figure 4 (e, f), which suggested the presence of largely pyrrolic peak at 399.4 eV, followed by other peak at 398.8 eV, which could be assigned due to the pyridinic N. However, no peak corresponding to 400.9 eV is observed, suggesting the absence of any graphitic N sites.^[15] Furthermore, the N (1s) spectrum of Pt-POP- SO_3H depicts positive shift of pyrrolic (0.3 eV) and pyridinic (0.5 eV) sites as compared to Pt-POP, shown in Figure 4 g and h. This result suggested the interaction

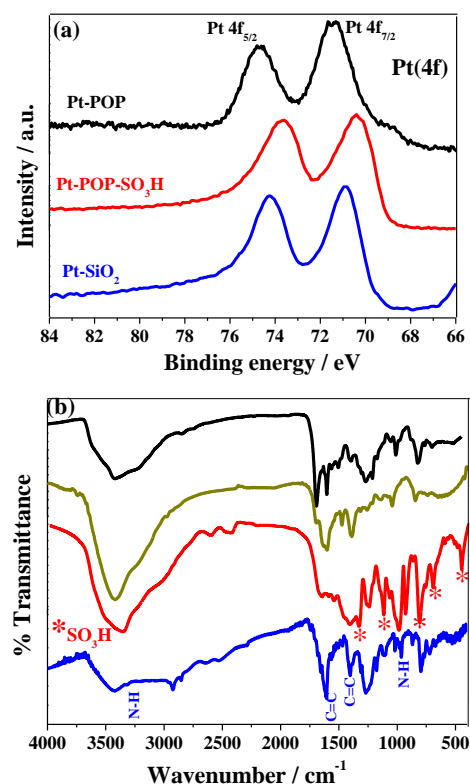


Figure 5. Pt 4f XPS spectra of Pt-POP, Pt-POP- SO_3H and Pt/SiO₂ (a); FT-IR spectra of tetraphenyl porphyrin (blue), Pt-POP- SO_3H (red), Pt-POP (dark yellow) and porphyrin functionalized polymer (black) (b).

between porphyrin and grafted acid groups. Again upon deconvolution, N1s of Pt-POP-SO₃H showed a broad shoulder at 397.2 eV, which could be assigned to the unprotonated pyridinic sites of porphyrin. This XPS result revealed higher pyrrolic to pyridinic N in Pt-POP than in Pt-POP-SO₃H, which justifies the decrease in free porphyrin sites in Pt-POP-SO₃H. It is pertinent to mention that observed iron content (Fe = 0.001 mmol g⁻¹ by ICP analysis) is extremely low in our Pt-POP samples and thus we did not observe any Fe 2p XPS spectrum.

The electronic properties of Pt NPs in Pt-POP and Pt-POP-SO₃H were investigated and compared with that of Pt/SiO₂. These results are shown in Figure 5a. The spectra contain a doublet peak having low energy band (Pt 4f_{7/2}) and a high energy band (Pt 4f_{5/2}) which correspond to Pt⁰ states. For Pt-POP, Pt binding energies (BEs) appear at 71.5 and 74.6 eV, which are ascribed to Pt in zero oxidation state and the B.E values showed close resemblance with Pt on other porphyrin supports.^[16] The B.E of Pt in Pt-POP showed positive shift when compared with Pt/SiO₂ (4f_{7/2} = 71.0 eV, Figure 5a) and Pt/C (4f_{7/2} = 71.1 eV).^[17] Taking into account on similar morphology and the particle size of Pt NPs, this change in B.E values may be ascribed to metal-support interaction that could be originated between nitrogen-sites of POP and Pt.^[18] Interestingly this metal-support interaction provides stabilization effect on Pt NPs.^[19] On the other hand, BEs of Pt (4f) in Pt-POP-SO₃H appears at 70.4 (4f_{7/2}) and 73.7 (4f_{5/2}) eV, which is ~(-0.9 eV) lower compared to Pt-POP. The large negative shift of the d-band centre of Pt is could be attributed to the interaction between Pt and the grafted acids. It is worth mentioning that electronegative sulfonic acids may donate electrons to Pt, resulting in large negative shift.^[20] Therefore Pt (4f) XPS result suggested significantly strong metal-support interaction.

Furthermore, CO chemisorption experiment suggested that Pt dispersion in Pt-POP is ~28%, which is partially diminishes to ~24% with Pt-POP-SO₃H because of some blocking with grafted acids. The values of Pt dispersibility in these catalysts are somehow comparable with Pt NPs deposited on other supports.^[21] This result suggested that these catalysts may be extended as hydrogenation catalyst. On the other hand, from FT-IR spectroscopic analysis we can easily distinguish between Pt-POP and Pt-POP-SO₃H. Figure 5b showed the sharp peak centered at 3415 cm⁻¹ is associated with stretching vibration of N-H sites present in porphyrin, which becomes broad and shifted to 3364 cm⁻¹ for Pt-POP-SO₃H on account of the -OH stretching in -SO₃H. The existence of porphyrin ring is confirmed from the appearance of bands at 1268, 1172 cm⁻¹ in Pt-POP-SO₃H and 1255, 1138 cm⁻¹ in Pt-POP that corresponds to pyrrole C-N stretching. Additionally bands at 1658, 1440 cm⁻¹ in Pt-POP-SO₃H and 1618, 1392 cm⁻¹ in Pt-POP are responsible to phenyl C=C stretching of the porphyrin.^[22] Nevertheless, the porphyrin functionality in Pt-POP and Pt-POP-SO₃H has close resemblance with C=C, N-H and C=N stretching vibration of free tetraphenyl porphyrin and the porphyrin polymer^[8a] as shown in Figure 5b. Sulfonic acid group in Pt-POP-SO₃H can be demonstrated by the appearance of bands at 467 and 1344 cm⁻¹, which corresponds to the symmetric and asymmetric C-S and C-SO₃H stretching vibrations, respectively.^[23] Again, the S-O stretching bands are observed at 831 and 710 cm⁻¹, whereas the bands at 1350, 1076 and 1126 cm⁻¹ can be assigned to asymmetric and symmetric vibrational absorption bands of -SO₃H.^[24] Therefore, from the FT-IR and XPS spectroscopic results, we can confirm the grafting of -SO₃H

sites and the successful formation of Pt-POP and Pt-POP-SO₃H.

2. Hydrogenation of 4-nitrostyrene

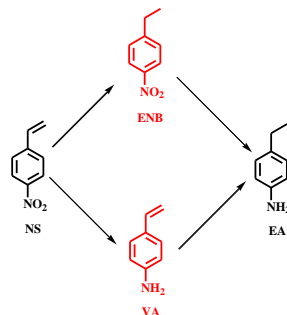
Initially the catalytic performance of Pt-POP was investigated for hydrogenation of 4-nitrostyrene as model reaction. In Table 1 we have shown several hydrogenation products of 4-nitrostyrene (NS), which are 4-ethylnitrobenzene (ENB), 4-vinyl aniline (VA) as partial hydrogenated products and 4-ethylaniline (EA) after complete hydrogenation. Highest selectivity (100%) to 4-ethylnitrobenzene is observed for 75% conversion of 4-nitrostyrene at 60 °C taking substrate/catalyst (S/C) ratio 9 (Table 1, entry 1). While decreasing S/C to 4.5, conversion of 4-nitrostyrene increases but the selectivity of 4-ethylnitrobenzene decreases (Table 1, entry 2). It is seen that when (S/C) is 3, 4-nitrostyrene exhibits full conversion (100%) to 4-ethylnitrobenzene (80%) and 4-ethylaniline (20%) (Table 1, entry 3). Therefore, from our experimental results we can conclude that at higher catalyst to substrate ratio, selectivity of the desired product (ENB) decreases and the probability of other hydrogenation product increases, although the substrate showed higher conversion efficiency. At high temperature (100 °C) and pressure (20 atm), selectivity to 4-ethylnitrobenzene decreases and 95% product becomes completely hydrogenated (Table 1, entry 4), indicating that Pt-POP is suitable to work only at low temperature and pressure. In this regard it is noteworthy to mention that heterogeneous supports with metallic NPs catalyzed hydrogenation of olefins in the presence of nitro group is limited in literatures. Considering this, the report of Sajiki and co-workers for Pd/Zelite (MS-3A, MS-5A) composites provide valuable understanding for the selective hydrogenation of 4-nitrostyrene to 4-ethylnitrobenzene.^[25] Among other NPs based polymer supports, Haruta and co-workers reported the activation of Pd on a conjugated porous polymer to monitor the selective conversion of 4-nitrostyrene to 4-ethyl nitrobenzene.^[26] Again, Garcia and others showed the utilization of Pd and Au NPs on adamantane-based covalent organic frameworks for selective conversion of 4-nitrostyrene to 4-ethylnitrobenzene.^[27] Further, reports on Pd NPs supported over porous spirobifluorene framework also suggested the advantage of porous polymers as active catalyst for selective reduction of 4-nitrostyrene to 4-ethylnitrobenzene.^[28] All these results suggested the superiority of porous organic framework as selective and stable support for the hydrogenation reaction.^[4b,29]

We have compared the catalytic performance of Pt-POP with conventional Pt/C support, which showed very low selectivity to 4-ethylnitrobenzene (40%) under almost similar hydrogenation reaction conditions (Table 1, entry 7). This comparison indicates that Pt/C is not chemoselective for C=C or -NO₂. While investigating the solvent effect for this reaction, we see that, polar solvents facilitate the hydrogenation compared to the non-polar solvents that might be because of the poor dispersibility of catalyst in non-polar solvent and low solubility of H₂ (Table 2). Kinetic investigation for NS hydrogenation is given in Figure 6a. Over Pt-POP, with increasing time, the concentration of 4-ethylnitrobenzene was continuously increased compared with other products. At 30 min reaction, complete conversion of NS is observed along with ENB (80%) and EA (20%), but we did not see traces of VA. Interestingly selectivity to ENB is not hampered throughout the course of the reaction and it attained high selectivity (~87%) after 20 min reaction for 80% conversion of NS. This

result suggested the selective reduction of alkene moiety of the NS over Pt-POP by suppressing the reactive nitro and benzene rings.

From our preliminary results we found that Pt-POP can be very useful for one step selective conversion of NS to ENB, which later encourages us to tune the metal-support interaction in switching of the product selectivity in favor of VA. Although POPs are used as catalyst for the hydrogenation reaction but their scope in chemoselective reductions^[30] rarely

Table 1. Hydrogenation of 4-nitrostyrene ^[a]



Entry	Catalyst	S/C	T / °C	P / atm	% Conv. ^[b]	% Sel. ^[b]		
						ENB	EA	VA
1	Pt-POP	9	60	10	75	100	-	-
2	Pt-POP	4.5	60	10	86	87	13	-
3	Pt-POP	3	60	10	100	80	20	-
4	Pt-POP	9	100	20	100	5	95	-
5	Pt/C ^[c]	3	60	10	100	15	85	-
6	Pt/C ^[c]	3	100	10	100	-	100	-
7	Pt/C ^[c,d]	3	60	10	80	40	60	-

^[a]0.5 mL THF, 30 min reaction time; ^[b]Calculated on the basis of GC analysis; ^[c]0.5 wt% on activated carbon having 700 m² g⁻¹ BET surface area; ^[d]Reaction at 15 min.

Table 2. Solvent effect of 4-nitrostyrene hydrogenation^[a]

Entry	Solvent	% Conv.	% Sel.		
			ENB	EA	AS
1	Water	50	32	26	42
2	Ethanol	100	60	40	-
3	2-propanol	70	86	14	-
4	Toluene	10	100	-	-
5	n-hexane	5	100	-	-
6	Dichloromethane	20	100	-	-
7	CHCl ₃	15	100	-	-

^[a] 60 °C, 10 atm H₂ for 30 min, 0.02 g 4-nitrostyrene, Pt-POP (0.02 g; 2 wt% Pt/Porphyrin).

studied. Thus, we assume that our surface-modified catalyst could exhibit better selectivity to 4-vinylaniline, which is a very important pharmaceutical product and is difficult to obtain in a single step from 4-nitrostyrene. In view of such catalytic

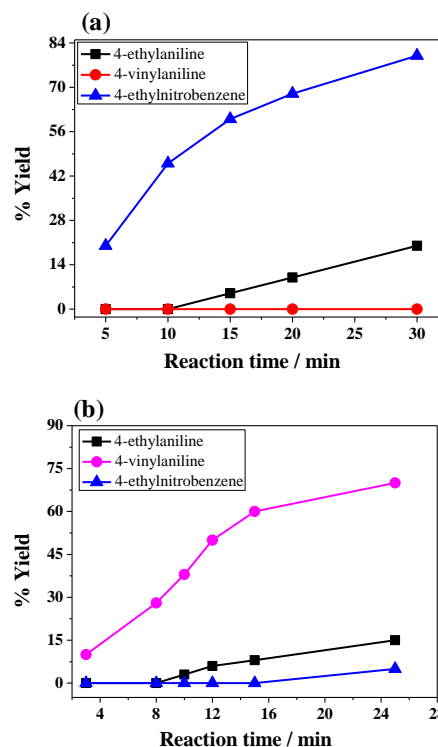
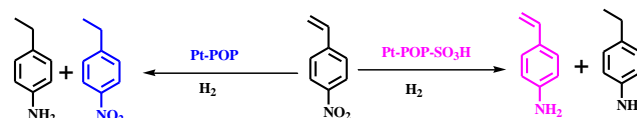


Figure 6. Kinetics for the hydrogenation of 4-nitrostyrene catalyzed by Pt-POP (a) and Pt-POP-SO₃H (b). Reaction condition: Subs/Cat = 3, 60 °C, 10 atm H₂, 0.5 mL THF.

challenges, previously phosphine, organic thiols are usually impregnated on the support to control the activity and selectivity of NPs.^[31] In this study, we prepare covalently grafted modifier on Pt-POP to understand the inversion of selectivity in nitrostyrene hydrogenation reactions and the results are shown in Figure 6b. Pt-POP-SO₃H material showed reverse selectivity compared to the pristine Pt-POP catalyst and the primary product of the hydrogenation is 4-aminostyrene. Figure 6b indicates the growth of 4-vinylaniline with time and at 15 min, 60% yield of 4-vinylaniline (85% selectivity) is observed along with 10% of 4-ethylaminobenzene. However, extending the reaction beyond 20 min, 4-vinylaniline, 4-ethylnitrobenzene and 4-ethylaminobenzene all are produced. At the end of 25 min, 70% vinylaniline, 16% ethylaniline and 6% ethylnitrobenzene are formed, and the selectivity in VA is still 76%. Nevertheless, at 25 min, VA selectivity decreases and after 1 h, EA is exclusively produced as complete hydrogenated product.

The difference in selectivity between Pt-POP and acid modified Pt-POP-SO₃H could be attributed to the partial blockage in the surfaces of Pt sites by sulfonic acids because Pt dispersibility on Pt-POP-SO₃H is lower (~24%) than that of

Pt-POP (28%).^[32] Hence, adsorption of substrates on the blocked sites of Pt in Pt-POP-SO₃H could be different than Pt-POP. On the other hand, from deconvoluted XPS spectra (Figure 7), we can also understand the difference in Pt⁰/Pt²⁺ ratio which could control the metal-support interaction and hence the selectivity. Pt 4f spectra in Figure 7, can split into several peaks as 70.4 (4f_{7/2}), 71.4 (4f_{7/2}), 73.6 (4f_{5/2}) and 74.6 eV (4f_{7/2}) for Pt(0) species and also 71.8 (4f_{7/2}) and 75.2 (4f_{5/2}) for Pt²⁺ species. The XPS result indicated higher Pt⁰/Pt²⁺ ratio in Pt-POP-SO₃H than Pt-POP, possibly because of interaction between metal and host. Nevertheless, the incorporated acid sites can strongly interact with the neighboring metal and induce changes in electronic and geometric structure of the support.^[33] Regarding this, the strong acidity of sulfonic acid close to Pt NPs should control the adsorption of NS molecules *via* hydrogen bonding with polar nitro groups and facilitate its adsorption. As a result nitro groups are more likely hydrogenated than vinyl groups, as seen with Pt-POP-SO₃H catalyst.^[34] Moreover the surface polarity induced by sulfonic acid may also trigger the preferential adsorption of more polar groups like -NO₂ than vinyl, as seen by others.^[9a] Since nitrobenzene hydrogenation is a surface sensitive reaction, therefore after grafting acid sites with Pt-POP, the geometry of the support may change, which sets up a competitive adsorption between flat and vertical modes of NS.^[35] Thus, the covalently attached sulfonic acid with Pt-POP possibly prevents the flat adsorption of 4-nitrostyrene substrate, resulting in the observed switch in selectivity.

Considering recyclability of the catalyst in nitrostyrene hydrogenation, we showed that both Pt-POP and Pt-POP-SO₃H can be recycled for at least three times without loss of much activity and selectivity. Again, hot filtration test and ICP-AES analysis of the filtrate after the reaction confirmed the absence of any Pt, thus eliminating the idea of leaching of the active sites from the catalyst. This experiment suggests that our supported Pt catalyzed reactions are heterogeneous in nature.

3. Hydrogenation of acetophenone

The successful use of Pt-POP as hydrogenation catalyst for reduction of 4-nitrostyrene encouraged us to extend the scope of this catalyst for reduction of acetophenone to 1-phenylethanol (A), because one-step acetophenone hydrogenation to 1-phenylethanol is difficult and it is accompanied by several by-products like cyclohexylethanone (B), and 1-cyclohexylethanol (C), as shown in Scheme 2. When Pt/SiO₂ was used as catalyst, the selectivity to A was only 33% at the conversion level of 20%. For commercially available Pt/C catalyst, the selectivity to A is 60% at the conversion of 89%. This result suggests that Pt-supported over silica and carbon materials are poor chemoselective towards A. However, Pt-POP showed high selectivity of about 95% towards the formation of A, with a conversion of 90%, which suggests that porphyrin-based solid support are effective in tailoring Pt NPs' activity towards hydrogenation of carbonyl compounds. As a control experiment, H₂PtCl₆/POP (prepared by impregnation of H₂PtCl₆ on the porphyrin support without reduction) showed no catalytic activity for acetophenone hydrogenation. This result apparently suggested the role of Pt in this reaction. The kinetics for this reaction is shown in Figure 8, suggesting that the reaction is fast at the beginning without having any induction period and after 3 h it reaches 90%

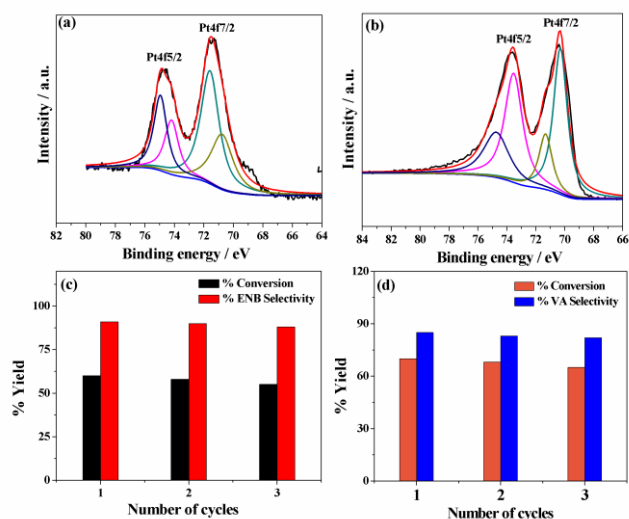
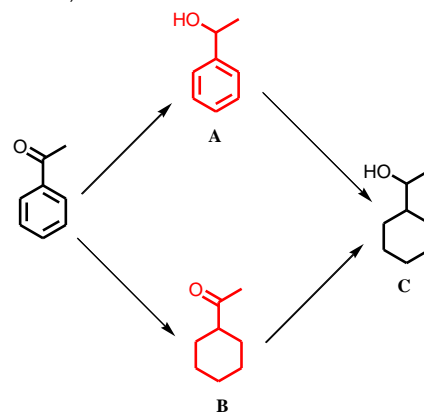


Figure 7. Deconvoluted Pt 4f XPS spectra of (a) Pt-POP and (b) Pt-POP-SO₃H; Recyclability test of Pt-POP (c, Subs/Cat = 3, 60 °C, 10 atm H₂, 0.5 mL THF for 15 min) and Pt-POP-SO₃H (d, Subs/Cat = 3, 60 °C, 10 atm H₂, 0.5 mL THF for 25 min)



Scheme 2. Possible hydrogenation products of acetophenone

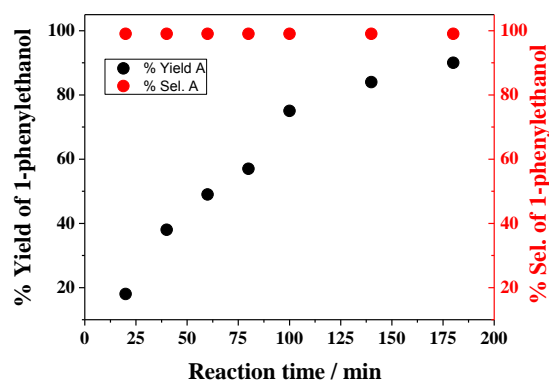


Figure 8. Reaction kinetics for Pt-POP catalyzed hydrogenation of acetophenone to 1-phenylethanol (0.015 g acetophenone, 0.010 g 2 wt% Pt-POP, 3 MPa H₂ and 100 °C temperature).

conversion and highest selectivity (95%) for A, beyond that although conversion increases, but at the same time the selectivity slowly decreases. In order to find out any leaching of Pt from the support, we have separated the catalyst from the reaction mixture after the end of 1 h reaction, and the reaction was continued without any catalyst. We found that the yield of A remains constant and did not increase after 1 h, which

demonstrated that the reaction is indeed catalyzed by solid Pt-POP instead of leached Pt metal.

Conclusion

In summary, we showed here that Pt nanoparticles supported over porous porphyrin nanospheres can act as stable heterogeneous catalyst for selective hydrogenation of 4-nitrostyrene and acetophenone. A switch in chemoselectivity of 4-nitrostyrene hydrogenation is observed after acid modification with Pt-porphyrin support. Therefore unlike Pt-POP, the acid modified catalyst showed high yield and selectivity for 4-aminostyrene, which could be either because of the existence of partially interacted Pt NPs at the surfaces or having different Pt⁰/Pt²⁺ ratio. The tunable chemoselectivity in the reduction of 4-nitrostyrene employing the surface functionalization strategy reported herein could endow considerable scientific interest in finding clean and cost-effective way for the synthesis of other important hydrogenated products.

Experimental Section

Chemicals and reagents

All reagents were of analytical grade and used as received unless otherwise stated. Terephthaldehyde, H₂PtCl₆, 4-nitrostyrene, acetophenone were purchased from Sigma-Aldrich, USA and used without any purification. Pyrrole was obtained from SRL, India and distilled under N₂ prior used. Glacial acetic acid and other remaining organic solvents were purchased from SRL, India and used after purification.

Instrumentation

Porosity measurement was carried out through the N₂ adsorption-desorption analysis at -196 °C by using Micromeritics ASAP2020 adsorption analyzer. Prior to the measurement, the samples were degassed at 120 °C for 4 h. BET surface area was measured within 0-0.18 P/P₀ ranges. Thermogravimetry analysis (TGA) was done by NETZSCH STA 449F3 analyzer in the temperature range 30-800 °C with a heating rate of 10 °C min⁻¹ in air. X-ray photoelectron spectroscopy (XPS) was recorded on a VG ESCALAB MK2 apparatus, using AlK α (h ν = 1486.6 eV) as the excitation source. Fourier transform infrared spectra (FT-IR) were recorded on a Nicolet Nexus 470 IR spectrometer. Chemical analysis was conducted on PLASAMSPEC-II inductively coupled plasma atomic emission spectrometry (ICP-AES). Powder X-ray diffraction was done on a RigakuD/Max2500 PC diffractometer with Cu K α radiation (λ =1.5418 Å) over the 2 θ range of 5–80° at a scan speed of 5° per min at room temperature. Bruker DPX-300 NMR spectrometer was used to measure ¹H and ¹³C NMR of the catalytic products (liquid state). Transmission electron microscopy (TEM) experiment was performed using HITACHI HT7700 at an acceleration voltage of 100 kV. Particle size was measured by randomly counting 100 nanoparticles based on HR-TEM images. CO chemisorption measurement was performed using Quantachrome Autosorb-1/C chemisorb apparatus at 40 °C temperature.

Synthesis of Pt-POP

Porphyrin functionalized porous polymer was reproduced from our prior report, using aromatic electrophilic substitution reaction between pyrrole and terephthaldehyde.^[8Error! Bookmark not defined.a] The resulting POP material was used to load Pt using conventional impregnation-reduction method. In a typical synthesis approach, 0.2 g POP powder was dispersed in 4 mL distilled water, followed by the addition of 400 μ L of 0.1 M H₂PtCl₆ solution. Then the mixture was centrifuged for 15 min to homogenize the solution and later stirred for an additional 12 h. Next, freshly prepared NaBH₄ aqueous solution (20 equivalents to Pt) was slowly added to the ice cold solution containing fine dispersion of Pt-POP and the mixture was stirred vigorously for another 6 h. Then the suspension was centrifuged, washed with water, ethanol and dried under vacuum. The solid product was designated as Pt-POP. Fe amount in Pt-POP was found to be ~0.001 mmol g⁻¹, as determined from Inductively Coupled Plasma Atomic Emission Spectroscopy.

Synthesis of Pt-POP-SO₃H

Porphyrin based POP was functionalized with sulfonic acid groups before loading with Pt nanoparticles. For this, 0.2 g POP was taken in a round bottom flask and dispersed in 5 mL CHCl₃. The solution was stirred in a magnetic stirrer and to it 100 μ L chlorosulfonic acid (ClSO₃H) was slowly added. Next, the solution was kept at 25 °C and continuously stirred for another 24 h. At the end, the solid product was collected by filtration and thoroughly washed with water and ethanol until the filtrate shows neutral (examine by pH paper). -SO₃H grafted POP was thus collected and used for the loading with Pt as mentioned before.

Hydrogenation of 4-nitrostyrene

The desired amount of Pt catalyst (0.02 g; Pt) was taken in an ampoule tube followed by the addition of 4-nitrostyrene at different substrate/catalyst ratio. Then 0.5 mL THF was added and the ampoule was transferred into a stainless-steel autoclave, sealed and flushed with H₂ three times to remove air from inside the autoclave and then pressurized to 10-20 atm H₂. The autoclave was then heated in an oil bath at 60-100 °C under continuous stirring. After 30 min reaction, excess H₂ was carefully discharged and the solid catalyst was separated by centrifugation. The filtrate was collected and diluted with ethanol, then analyzed by using an Agilent 7890 GC instrument equipped with an Agilent J&W GC HP-5 capillary column (30 m x 0.32 mm x 0.25 mm).

Acetophenone hydrogenation

Pt-POP catalyst (0.010 g) was added to an ampoule tube, followed by the addition of acetophenone (0.015 g). The ampoule tube was then transferred into a stainless-steel autoclave, sealed and flushed with H₂ three times to remove air from inside the autoclave, and then pressurized to 3 MPa H₂. The autoclave was then heated on an oil bath at 100 °C under stirring. After 2 h, the remaining H₂ was carefully discharged and the solid catalyst was separated by centrifugation. The filtrate was collected and diluted with ethanol, then analyzed by using an Agilent 7890 GC

instrument equipped with an Agilent J&W GC HP-5 capillary column (30 m x 0.32 mm x 0.25 mm).

Acknowledgements

AM thanks S. N. Bose National Centre for Basic Sciences, India for providing him generous support. AB thanks DST, New Delhi for providing Indo-Egypt international project grant.

Keywords: Porous organic polymer; porphyrin network, Sulfonic acid modification, Hydrogenation reaction, Selective reduction.

- [1] a) R. J. White, R. Luque, V. L. Budarin, J. H. Clark, D. J. Macquarrie, *Chem. Soc. Rev.* **2009**, *38*, 481-494; b) A. Modak, J. Sun, W. Qiu, X. Liu, *Catalysts* **2016**, *6*, 161-172; c) C. M. Marrodan, F. Liguori, P. Barbaro, S. Caporali, L. Merlo, C. Oldani, *ChemCatChem* **2017**, *9*, 4256-4267; d) F. Xie, R. Xie, J. X. Zhang, H. F. Jiang, L. Du, M. Zhang, *ACS Catal.* **2017**, *7*, 4780-4785; e) F. Xie, Q. H. Chen, R. Xie, H. F. Jiang, M. Zhang, *ACS Catal.* **2018**, *8*, 5869-5874; f) W. H. Li, C. Y. Li, H. Y. Xiong, Y. Liu, W. Y. Huang, G. J. Ji, Z. Jiang, H. T. Tang, Y. M. Pan, Y. J. Ding, *Angew. Chem. Int. Ed.* **2019**; DOI: 10.1002/anie.201814493.
- [2] J. C. Matsubu, S. Y. Zhang, L. DeRita, N. S. Marinkovic, J. G. G. Chen, G. W. Graham, X. Q. Pan, P. Christopher, *Nature Chem.* **2017**, *9*, 120-127.
- [3] a) J. B. Ernst, C. Schwermann, G. Yokota, M. Tada, S. Muratsugu, N. L. Doltsinis, F. Glorius, *J. Am. Chem. Soc.* **2017**, *139*, 9144-9147; b) S. Jayakumar, A. Modak, M. Guo, H. Li, X. Hu, Q. Yang, *Chem. Eur. J.* **2017**, *23*, 7791-7797.
- [4] a) S. Yun, S. Lee, S. Yook, H. A. Patel, C. T. Yavuz, M. Choi, *ACS Catal.* **2016**, *6*, 2435-2442; b) P. Bhanja, X. Liu, A. Modak, *ChemistrySelect* **2017**, *2*, 7535-7543.
- [5] a) H. Liu, L. Chang, L. Chen, Y. Li, *ChemCatChem* **2016**, *8*, 946-951; b) W. J. Chen, B. H. Cheng, Q. T. Sun, H. Jiang, *ChemCatChem* **2018**, *10*, 3659-3665.
- [6] a) Y. Zhang, S. N. Riduan, *Chem. Soc. Rev.* **2012**, *41*, 2083-2094; b) A. Modak, A. Bhaumik, *ChemistrySelect* **2016**, *6*, 1192-1200; c) A. Modak, P. Bhanja, A. Bhaumik, *Chem. Eur. J.* **2018**, *24*, 14189-14197; d) W. H. Li, C. Y. Li; L. Yan, H. T. Tang, H. S. Wang, Y. M. Pan, Y. J. Ding, *Chem. Commun.* **2018**, *54*, 8446-8449; e) W. Tong, W. H. Li, Y. He, Z. Y. Mo, H. T. Tang, H. S. Wang, Y. M. Pan, *Org. Lett.* **2018**, *20*, 2494-2498; f) P. Bhanja, A. Modak, A. Bhaumik, *ChemCatChem* **2019**, *9*, 244-257.
- [7] a) J. Liu, Y. Gao, D. Cao, L. Zhang, Z. Guo, *Langmuir* **2011**, *27*, 7926-7933; b) S. Lin, M. R. Wiesner, *Environ. Sci. Technol.* **2012**, *46*, 13270-13277; c) D. Spagnoli, J. F. Banfield, S. C. Parker, *J. Phys. Chem. C* **2008**, *112*, 14731-14736.
- [8] a) A. Modak, M. Nandi, J. Mondal, A. Bhaumik, *Chem. Commun.* **2012**, *48*, 248-250; b) A. Modak, M. Pramanik, S. Inagaki, A. Bhaumik, *J. Mater. Chem. A* **2014**, *2*, 11642-11650.
- [9] a) M. Makosch, W. I. Lin, V. Bumbálek, J. Sá, J. W. Medlin, K. Hungerbühler, J. A. van Bokhoven, *ACS Catal.* **2012**, *2*, 2079-2081; b) C. Bergerand, A. Yarulin, F. C. Lizana, J. Wärnå, E. Sulman, D. Y. Murzin, L. Kiwi-Minsker, *Ind. Eng. Chem. Res.* **2015**, *54*, 8659-8669; c) Y. Tan, X. Y. Liu, L. Zhang, A. Wang, L. Li, X. Pan, S. Miao, M. Haruta, H. Wei, H. Wang, F. Wang, X. Wang, T. Zhang, *Angew. Chem. Int. Ed.* **2017**, *56*, 2709-2713.
- [10] A. S. Campisi, C. E. Chan-Thaw, A. Villa, *Appl. Sci.* **2018**, *8*, 1159.
- [11] a) Y. Zhou, J. A. Switzer, *J. Alloys Comp.* **1996**, *237*, 1-5; b) A. Modak, A. Bhaumik, *J. Mol. Catal. A: Chem.* **2016**, *425*, 147-156.
- [12] a) W. Shi, K. H. Wu, J. Xu, Q. Zhang, B. Zhang, D. S. Su, *Chem. Mater.* **2017**, *29*, 8670-8678; b) V. Sadhasivam, R. Balasaravanan, C. Chithiraikumar, A. Siva, *ChemCatChem* **2018**, *10*, 3833-3844.
- [13] a) J. F. Moulder, W. F. Stickle, P. E. Sobol, K. D. Bomben, Handbook of X-Ray Photoelectron Spectroscopy: A Reference Book of Standard Spectra for Identification and Interpretation of XPS Data, Physical Electronics, USA, 1995; b) B. J. Lindberg, K. Hamrin, G. Johansson, U. Gelius, A. Fahlman, C. Nordling, K. Siegbahn, *Phys. Scr.* **1970**, *1*, 286; c) Q. Guan, Y. Li, Y. Chen, Y. Shi, J. Gu, B. Li, R. Miao, Q. Chena, P. Ning, *RSC Adv.* **2017**, *7*, 7250-7258.
- [14] F. Moulder, W. F. Stickle, P. E. Sobol, K. D. Bomben, Handbook of X-Ray Photoelectron Spectroscopy: A Reference Book of Standard Spectra for Identification and Interpretation of XPS Data, Physical Electronics, USA, 1995.
- [15] D. M. Sarno, L. J. Matienzo, W. E. Jones, Jr, *Inorg. Chem.* **2001**, *40*, 6308-6315.
- [16] G. Geng, Z. Wang, P. Chen, B. Guan, C. Yang, M. Liu, *Phys. Chem. Chem. Phys.* **2018**, *20*, 8488-8497.
- [17] W. D. Lee, D. H. Lim, H. J. Chun, H. I. Lee, *Int. J. Hydrogen Energy* **2012**, *37*, 12629-12638.
- [18] X. Zhao, J. B. Zhu, L. Liang, J. H. Liao, C. P. Liu and W. Xing, *J. Mater. Chem.* **2012**, *22*, 19718-19725; b) R. X. Wang, J. J. Fan, Y. J. Fan, J. P. Zhong, L. Wang, S. G. Sun, X. C. Shen, *Nanoscale* **2014**, *6*, 14999-15007.
- [19] S. Mayavan, H. S. Jang, M. J. Lee, S. H. Choi, S. M. Choi, *J. Mater. Chem. A* **2013**, *1*, 3489-3494.
- [20] J. Lu, Y. Li, S. Li, S. P. Jiang, *Sci. Rep.* **2016**, *6*, 21530-21542.
- [21] T. L. M. Rossi, J. L. Fiorio, M. A. S. Garcia, C. P. Ferraz, *Dalton Trans.* **2018**, *47*, 5889-5915.
- [22] Z. Guo, F. Du, D. Ren, Y. Chen, J. Zheng, Z. Liu, J. Tian, *J. Mater. Chem.* **2006**, *16*, 3021-3030.
- [23] H. Yu, Y. Jin, Z. Li, F. Peng, H. Wang, *J. Solid State Chem.* **2008**, *181*, 432-438.
- [24] J. R. M. N. Kalla, M. R. Kim, I. Kim, *Ind. Eng. Chem. Res.* **2018**, *57*, 11583-11591.
- [25] T. Maegawa, T. Takahashi, M. Yoshimura, H. Suzuka, Y. Monguchi, H. Sajiki, *Adv. Synth. Catal.* **2009**, *351*, 2091-2095.
- [26] T. Ishida, Y. Onuma, K. Kinjo, A. Hamasaki, H. Ohashi, T. Honma, T. Akita, T. Yokoyama, M. Tokunaga, M. Haruta, *Tetrahedron*, **2014**, *70*, 6150-6155.
- [27] M. M. Trandafir, L. Pop, N. D. Hădăde, M. Florea, F. Neațu, C. M. Teodorescu, B. Duraki, J. A. van Bokhoven, I. Grosu, V. I. Parvulescu, H. Garcia, *Catal. Sci. Technol.* **2016**, *6*, 8344-8354.
- [28] M. M. Trandafir, L. Pop, N. D. Hădăde, I. Hristea, C. M. Teodorescu, F. Krumeich, J. A. van Bokhoven, I. Grosu, V. I. Parvulescu, *ChemCatChem* **2018**, *10*, DOI: 10.1002/cctc.201801247.
- [29] Z. C. Ding, C. Y. Li, J. J. Chen, J. H. Zeng, H. T. Tang, Y. J. Ding, Z. P. Zhan, *Adv. Synth. Catal.* **2017**, *359*, 2280-2287.
- [30] L. Li, H. Zhao, R. Wang, *ACS Catal.* **2015**, *5*, 948-955.
- [31] a) C. H. Lien, J. W. Medlin, *J. Phys. Chem. C* **2014**, *118*, 23783-23789; b) S. H. Pang, C. A. Schoenbaum, D. K. Schwartz, J. W. Medlin, *ACS Catal.* **2014**, *4*, 3123-3131; c) Q. Wu, B. Zhang, C. Zhang, X. Meng, X. Su, S. Jiang, R. Shi, Y. Li, W. Lin, M. Arai, H. Cheng, F. Zhao, *J. Catal.* **2018**, *364*, 297-307.
- [32] C.H. Bartholomew, *Appl. Catal. A* **2001**, *212*, 17.
- [33] C. H. Bartholomew, in: B. Delmon, G.F. Froment (Eds.), Catalyst Deactivation 1987, *Stud. Surf. Sci. Catal.*, Vol. 34, Elsevier, Amsterdam, **1987**.
- [34] A. K. Sharma, R. B. Sunoj, *J. Org. Chem.* **2012**, *77*, 10516-10524.
- [35] M. Boronat, A. Corma, *Langmuir* **2010**, *26*, 16607-16614.

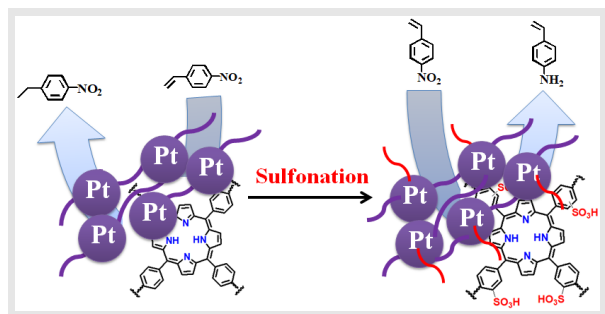
Received: ((will be filled in by the editorial staff))
Published online: ((will be filled in by the editorial staff))



Accepted Manuscript

Table of Content

FULL PAPER

**Chemoselective hydrogenation by supported Pt NPs.**

Pt nanoparticles supported over porous porphyrin nanosphere showed a switching in selectivity in the hydrogenation of 4-nitrostyrene via simple surface modification by grafted sulfonic acid groups. The acid modified catalyst showed higher selectivity for 4-aminostyrene, whereas pristine catalyst yielded 4-ethylnitrobenzene.

Arindam Modak,^{*,[a,b]} Piyali Bhanja and Asim Bhaumik^{*,[a]}

Pt Nanoparticles Supported over Porous Porphyrin Nanospheres for Chemoselective Hydrogenation Reactions

Accepted Manuscript